Propagation of electromagnetic waves in the plasma near electron cyclotron resonance: Undulator-induced transparency[a)]

G. Shvets[b)] and M. Tushentsov
Department of Physics and Institute for Fusion Studies, The University of Texas at Austin, One University Station, Austin, Texas 78712

M. D. Tokman and A. Kryachko
Institute of Applied Physics, Russian Academy of Sciences, Nizhny Novgorod 603950, Russia

(Received 22 November 2004; accepted 5 January 2005; published online 7 April 2005)

Propagation of electromagnetic waves in magnetized plasma near the electron cyclotron frequency can be strongly modified by adding a weak magnetic undulator. For example, both right- and left-hand circularly polarized waves can propagate along the magnetic field without experiencing resonant absorption. This effect of entirely eliminating electron cyclotron heating is referred to as the undulator-induced transparency (UIT) of the plasma, and is the classical equivalent of the well-known quantum mechanical effect of electromagnetically induced transparency. The basics of UIT are reviewed, and various ways in which UIT can be utilized to achieve exotic propagation properties of electromagnetic waves in plasmas are discussed. For example, UIT can dramatically slow down the waves' group velocity, resulting in the extreme compression of the wave energy in the plasma. Compressed waves are polarized along the propagation direction, and can be used for synchronous electron or ion acceleration. Strong coupling between the two wave helicities are explored to impart the waves with high group velocities $\partial\omega/\partial k$ for vanishing wave numbers k. Cross-helicity coupling for realistic density and magnetic field profiles are examined using a linearized fluid code, particle-in-cell simulations, and ray-tracing WKB calculations. © *2005 American Institute of Physics*. [DOI: 10.1063/1.1865053]

I. INTRODUCTION

Electromagnetically induced transparency (EIT) is a well known[1–4] in nonlinear optics phenomenon. Its main signature that lends EIT its name is the propagation of an electromagnetic wave through the normally opaque medium in the presence of a second, more powerful electromagnetic wave. For example, a medium consisting of three-level atoms schematically shown in Fig. 1 (where the levels 0, 1, and 2 are, respectively, the ground, excited, and Raman atomic levels with energies $\mathcal{E}_0$, $\mathcal{E}_1$, and $\mathcal{E}_2$), is opaque to an electromagnetic wave (probe) with frequency $\omega_1=(\mathcal{E}_1-\mathcal{E}_0)/\hbar$ tuned to the transition from the ground to the excited state. When the medium is illuminated by a second laser beam (pump) with frequency $\omega_0=(\mathcal{E}_1-\mathcal{E}_2)/\hbar$, it becomes transparent to the probe. In the parlance of atomic physics, transparency is achieved because the three-level atomic system evolves into the so-called trapped state, where atoms exist in a superposition of the ground and Raman states.[2] First predicted and observed in gasses, it was later extended to solids.[5,6]

Another remarkable property of the EIT media is their ability to dramatically slow down light.[7] Recent experiments demonstrated that light can be stopped, stored,[8,9] and even forced to move backwards[10] in the EIT medium. Slowing down is achieved because the photons of the original probe pulse are redistributed in the EIT medium between the propagating electromagnetic wave and the nonpropagating Raman excitation of the medium. The resulting so-called dark-state polaritons[11] can have a small electromagnetic energy content and, therefore, very low group velocity. A number of promising applications of EIT based on the slow light have been suggested.[12–14] For example, it has been suggested that strong coupling between electromagnetic and acoustic waves can be realized by slowing down light to the sound speed Matsko *et al.*[15]

It has recently been shown that EIT is possible not only in quantum mechanical systems (as previously thought), but also in classical systems such as the magnetized plasma[16–20] A right-hand circularly polarized (RHCP) electromagnetic wave launched along the magnetic field $\mathbf{B}=B_0\mathbf{e}_z$ and having the frequency $\omega_1=\Omega_0$ (where $\Omega_0=eB_0/mc$ is the electron cyclotron frequency) is resonantly absorbed by the plasma. This phenomenon, known as the electron cyclotron heating (ECH), occurs only for one of the two wave helicities because the electric field of the RHCP wave rotates in the same direction as the electrons in the magnetic field $B_0\mathbf{e}_z$. The other helicity corresponding to the left-hand circularly polarized (LHCP) wave propagates without absorption. Transparency of the plasma to RHCP wave can be achieved, and ECH overcome, by adding a lower-frequency pump[16,17] with $\omega_0=\Omega_0-\omega_p$, where $\omega_p=(4\pi e^2N/m)^{1/2}$ is the electron plasma frequency. Here N is the plasma frequency, $-e$ is the electron charge, and m is the electron mass. Given the unavoidable small inhomogeneity of the plasma density and magnetic field, as well as the finite plasma temperature, the required for transparency pump power is very high.

[a)]Paper FI2 6, Bull. Am. Phys. Soc. **49**, 138 (2004).
[b)]Invited speaker.

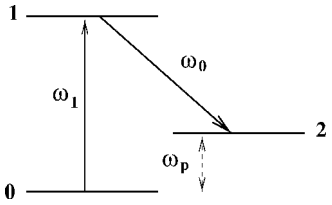

FIG. 1. Schematic of EIT in a three-level quantum mechanical system. Weak pulse with frequency $\omega_1=(\mathcal{E}_1-\mathcal{E}_0)/\hbar$ is absorbed in the absence of a pump. In the presence of a strong pump tuned to $\omega_0=\omega_1-\omega_p$ [where $\omega_p=(\mathcal{E}_2-\mathcal{E}_0)/\hbar$] medium becomes transparent. The three levels shown are the ground (labeled 0), excited (labeled 1), and Raman (labeled 2).

Fortunately, in the special case of $\Omega_0=\omega_p$ the frequency of the pump is equal to zero. This corresponds[17] to a magnetostatic undulator with $\mathbf{B}_u=B_u(\mathbf{e}_x \sin k_u z+\mathbf{e}_v \cos k_u z)$ as the pump. Because a high field magnetic undulator is relatively straightforward to make EIT can indeed by experimentally realized in that special regime referred to as the undulator induced transparency (UIT). Cyclotron absorption is suppressed because of the excitation of the longitudinal plasma wave (plasmon). Magnetostatic undulator couples the longitudinal plasma and the transverse RHCP waves resulting in a hybrid wave which has both longitudinal and transverse components of the electric field. The hybrid wave is not absorbed at the cyclotron frequency, which is the signature of the UIT of plasma. Because of the practically achievable axial and undulator magnetic field strengths B_0 and B_u, UIT is a microwave/plasma phenomenon with an upper frequency limit of about 300 GHz. A typical experimental setup for a UIT experiment is shown in Fig. 2; plasma column is immersed in axial magnetic field of a solenoidal magnet with a helical undulator field superimposed on it. High power microwaves from a gyrotron are injected into the plasma and compressed by a significant factor dependent on the magnetic field strengths of the undulator and solenoid.

The group velocity of the hybrid wave can be very slow for $B_u \ll B_0$ making the hybrid wave the equivalent of the slow light in quantum optics. The slowing down occurs because the hybrid wave is primarily longitudinally polarized and has a small Poynting vector. If the spatial length of the injected electromagnetic wave is $L_0=c\tau_0$ (where τ_0 is the temporal pulse duration), the spatial length of the hybrid wave is $L_1=v_g\tau_0 \ll L_0$, resulting in the energy density increase by a factor $G=L_0/L_1 \gg 1$. The hybrid nature of the slow wave in the plasma bears a strong similarity to the coupled excitations of the light and matter: the so-called dark-state polaritons.[11] The essential difference is that the slowing down of light due to creation of dark-state polaritons does not amount to energy compression: most of the compressed pulse energy is carried away by the pump, plus some is stored in atoms. In UIT the entire pulse energy is compressed.

One of the promising applications of the compressed energy in the plasma is the high-gradient acceleration of electrons and ions, made even more attractive by the ability to tune the phase velocity of the accelerating field.[19] Another possible application is to pulse chopping: if the group velocity of the wave could be rapidly changed (by, for example, changing the plasma density), then the initially long microwave pulse could be significantly shortened. These applications rely exclusively on the small group velocity of waves in UIT plasma, and they have been recognized in our earlier UIT work.[17,19] It turns out that the strong coupling between the two electromagnetic wave helicities (RHCP and LHCP) creates opportunities for engineering propagation properties of waves in the plasma as suited for other applications. For example, a helical undulator creates a significant asymmetry between forward and backward moving waves. One can then engineer the dispersion properties of the waves in such a way that the group velocity for a vanishing wave number k_z is not zero. Such waves can be used for extracting energy from relativistic electron beams at high efficiency.[21]

Interhelicity coupling also has a strong effect on the very possibility of the above mentioned energy compression. High energy compression requires a large reduction in the group velocity: $V_g/c \ll 1$. Earlier analytic models[16–18,20] neglected the possibility of interhelicity coupling by assuming that the hybrid wave is the combination of the transverse RHCP and longitudinal plasma waves. The analytic prediction of such single-helicity theory is that the group velocity of the hybrid wave (RHCP plus the electron plasma wave) is $v_g=(B_u/B_0)^2c/2$ (Ref. 17) regardless of the undulator period and helicity. Therefore, it is advantageous to achieve UIT with as small B_u as the plasma and magnetic field homogeneities allow. Earlier particle-in-cell (PIC) simulations[19] have confirmed UIT for $B_u \geqslant 0.5B_0$ but failed to find transparency for smaller values of B_u. Moreover, they revealed a peculiar and unaccounted for by the single-helicity analytic model dependence of the wave propagation on the undulator period and helicity.

In this work the interhelicity coupling is fully explored. The dependence of wave propagation in the UIT plasma on the undulator period and helicity are explained. Depending

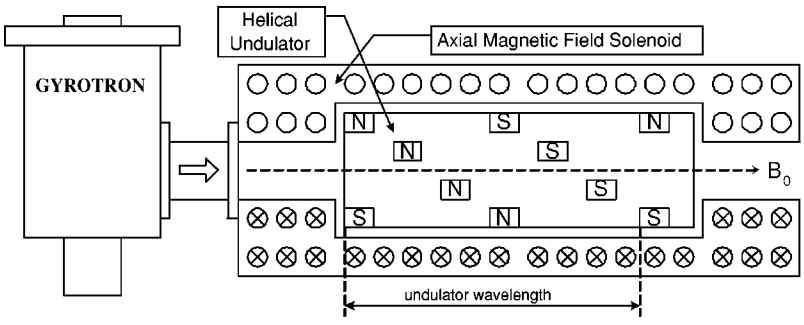

FIG. 2. Conceptual setup of a UIT experiment: plasma is immersed in a combination of the solenoidal and helical undulator magnetic fields. Microwaves at the electron cyclotron frequency are injected into and compressed in the plasma.

on the undulator period $\lambda_u=2\pi/k_u$, several propagation regimes are identified: (a) small-pitch $k_u \ll \Omega_0/c$, (b) intermediate-pitch $k_u \sim \Omega_0/c$, and (c) large-pitch $k_u \gg \Omega_0/c$. Moreover, it is found that the helical undulator removes the symmetry between the forward and backward propagating waves. The original single-helicity calculation is found valid only in the regime (c). Energy compression by almost two orders of magnitude is demonstrated in that regime using PIC simulations. In the regime (b), realized in the earlier PIC simulations,[19] plasma is indeed opaque for $B_u \ll B_0$ due to interhelicity coupling. The regime (a) holds interesting opportunities for engineering wave propagation properties near $k_z=0$, such as ensuring a nonvanishing group velocity.

The rest of the paper is organized as follows. In Sec. II linearized equations describing the coupling between the RHCP and LHCP electromagnetic waves are introduced and numerically integrated. They are also analyzed in the WKB approximation valid for smoothly varying plasma density and magnetic field. WKB (or ray-tracing) approach is a very convenient tool for predicting the crude features of wave propagation, such as whether the launched wave transmits through the plasma. In Sec. II B the three propagation regimes are analyzed. Engineering electromagnetic wave propagation properties in the plasma in the vicinity of $k_z=0$ are discussed in Sec. III. The results of PIC simulations of wave compression in the UIT plasma and discussion of their relevance to particle acceleration are presented in Sec. IV.

II. LINEAR EQUATIONS DESCRIBING INTERHELICITY COUPLING

A one-dimensional in space linear model of electromagnetic wave propagation in the UIT plasma is considered below. Ion motion is neglected, and plasma electrons are described as a cold linear fluid characterized by its velocity $\mathbf{v}$. Some of the nonlinear aspects of the UIT have been investigated[18] in the context of the single-helicity theory. Instead, coupling between different helicities (left- and right-hand circular polarizations) is fully accounted for in this section. The total magnetic field consists of the spatially varying axial $B_0(z)\mathbf{e}_z$ and transverse (undulating) $\mathbf{B}_u=B_u(\mathbf{e}_z \sin k_u z + \mathbf{e}_y \cos k_u z)$ fields. One can assign a pseudoscalar quantity $H=\mathbf{A}_u\cdot\mathbf{B}_u$ (where $\mathbf{B}_u=\boldsymbol{\nabla}\times\mathbf{A}_u$) to the undulator. Note that the helicity H changes sign with k_u. Thus, the helicity of a helical undulator can be reversed by reversing the sign of k_u. We refer to a helical undulator with $k_u>0$ as the positive-helicity undulator. Linearized fluid equations for the transverse and longitudinal components of the electron velocity are

$$\frac{\partial \mathbf{v}_\perp}{\partial t}+\Omega_0[\mathbf{v}_\perp\times\mathbf{e}_z]=-\frac{e}{m}\left(\mathbf{E}_\perp+\frac{v_z}{c}[\mathbf{e}_z\times\mathbf{B}_u]_\perp\right), \tag{1}$$

$$\frac{\partial v_z}{\partial t}=-\frac{e}{m}\left(E_z+\frac{1}{c}\mathbf{v}_\perp\times\mathbf{B}_u\right)_z. \tag{2}$$

Coupling of the transverse and longitudinal degrees of freedom through the magnetic undulator expressed by Eqs. (1) and (2) is essential making the plasma transparent at the cyclotron frequency.

Linearized wave equation for the electric field simplifies in the one-dimensional (1D) limit to $\partial_t E_z=(m/e)\omega_p^2 v_z$ for the longitudinal and $(c^2\partial_z^2-\partial_t^2)\mathbf{E}_\perp=-(m/e)\omega_p^2\partial_t\mathbf{v}_\perp$ for the transverse components. It is convenient to expand the transverse components of the electric field as the superposition of the right- and left-hand circularly polarized components: $e\mathbf{E}_\perp/(mc\omega)=\mathrm{Re}[(a_+\mathbf{e}_+ + a_-e_-)\exp(-i\omega t)]$. Expressing the electron fluid velocity in terms of the electric field and substituting it into the wave equation yields, after some algebra,[22] the equations describing interhelicity coupling:

$$\left[\frac{\partial^2}{\partial z^2}+\frac{\omega^2}{c^2}n_+^2(z)\right]a_+=\frac{\omega^2}{c^2}g(z)e^{2ik_u z}a_-, \tag{3}$$

$$\left[\frac{\partial^2}{\partial z^2}+\frac{\omega^2}{c^2}n_-^2(z)\right]a_-=\frac{\omega^2}{c^2}g(z)e^{-2ik_u z}a_+, \tag{4}$$

where the refractive indices $n_\pm$ for the RHCP and LHCP polarizations, respectively, are

$$n_\pm^2=1-\frac{\omega_p^2}{\omega}\frac{2\Omega_R^2\omega-(\omega^2-\omega_p^2)(\omega\pm\Omega_0)}{4\Omega_R^2\omega^2-(\omega^2-\omega_p^2)(\omega^2-\Omega_0^2)}, \tag{5}$$

the coupling coefficient g is

$$g=\frac{2\Omega_R^2\omega_p^2}{4\Omega_R^2\omega^2-(\omega^2-\omega_p^2)(\omega^2-\Omega_0^2)} \tag{6}$$

and the spatial dependencies of the refractive indices on z originates from the parametric dependence of $n_\pm$ on the spatially inhomogeneous plasma density and axial magnetic field. Without an undulator the expressions for refraction indices revert to the usual[23] formulas for the RHCP and LHCP waves propagating along the magnetic field in the plasma: $n_\pm^2=1-\omega_p^2/\omega(\omega\mp\Omega_0)$. Although $n_\pm$ are explicitly independent of k_u, wave propagation in the UIT does depend on k_u through Eqs. (3) and (4). The earlier studied single-helicity case corresponding to $g=0$ does not reveal any dependence of the wave propagation on the undulator wave number or helicity. Equations (3) and (4) describe coupling of the electromagnetic waves into a UIT plasma with arbitrary profiles of the plasma density and magnetic field. In the rest of the paper (except Sec. IV) we assume the following profiles: $N(z)/N_0=2\tanh(\omega z/5c-5)-2\tanh(\omega z/5c-19)$ and $B_0(z)/B_0=2-0.5\tanh(\omega z/5c-5)+\tanh(\omega z/5c-19)$. These profiles have constant density and magnetic field plateaus for $40<\omega z/2\pi c<70$. A "magnetic trap" profile of the axial magnetic is chosen to avoid resonances of $n_\pm$ at the entrance or exit of the plasma.

There exists a resonant relationship between the electron plasma and cyclotron frequencies that we refer to as the "perfect" transparency case: $\Omega_0=\overline{\omega}_p\equiv\sqrt{\omega_p^2+\Omega_R^2}$. When this condition is satisfied, and $\omega=\Omega_0=\overline{\omega}_p$, it is found that $n_+=1$ corresponding to perfect transparency. Note that the undulator slightly renormalizes the effective plasma frequency.[18] The refractive index of the RHCP wave in the perfect transparency case is approximately given by $n_+^2\approx 1+\omega_p^2\delta\omega/\omega(\Omega_R^2-\delta\omega^2)$, where $\delta\omega=\omega-\Omega_0$ is the detuning from the electron cyclotron resonance.

Because one of the most appealing applications of UIT is electron and ion acceleration in plasma,[17,19] we also present, for the reference, the expression for the longitudinal electric field:

$$E_z = \frac{mc\omega}{e} g\left(a_+ \frac{\omega+\Omega_0}{2\Omega_R} e^{-ik_u z} - a_- \frac{\omega-\Omega_0}{2\Omega_R} e^{ik_u z} \right) e^{-i\omega t} + \text{c.c.} \tag{7}$$

According to Eq. (7), the accelerating field under or close to UIT conditions ($\omega \approx \Omega_0$) is determined primarily by the RHCP amplitude a_+. Thus, the injected electromagnetic wave should have a significant RHCP component inside the plasma in order to excite a strong plasma wave.

A. WKB analysis of coupled wave propagation

While it is possible at this stage to solve Eqs. (3) and (4) numerically using the appropriate boundary conditions before the plasma start (incident RHCP wave of a given amplitude a_+^{inc}) and after the plasma end (only transmitted RHCP and LHCP), it is instructive to develop a qualitative understanding of wave propagation in the UIT plasma. Geometric optics can be used if plasma parameters vary smoothly on a scale of the radiation wavelength. Electromagnetic waves in the plasma can be described using phase-space trajectories in the (n,z) phase plane.[24] The resulting approximate description of the wave propagation is equivalent to the multicomponent WKB theory.[25,26] The WKB description assigns propagation trajectories in the (n,z) phase plane to different electromagnetic modes.

Before applying WKB to Eqs. (3) and (4), it is convenient to eliminate the rapidly oscillating in z coefficients in the right-hand sides by making the following substitution: $a_\pm = \tilde{a}_\pm \exp(\pm i n_u \tilde{z})$, where $\tilde{z} = \omega z/c$ and $n_u = k_u c/\omega$. After substituting $a_\pm$ into Eqs. (3) and (4), we obtain

$$\frac{\partial^2 \tilde{a}_+}{\partial \tilde{z}^2} + 2in_u \frac{\partial \tilde{a}_+}{\partial \tilde{z}} + (n_+^2 - n_u^2)\tilde{a}_+ = g\tilde{a}_-,$$

$$\frac{\partial^2 \tilde{a}_-}{\partial \tilde{z}^2} - 2in_u \frac{\partial \tilde{a}_-}{\partial \tilde{z}} + (n_-^2 - n_u^2)\tilde{a}_- = g\tilde{a}_+, \tag{8}$$

where all quantities slowly vary with $\tilde{z}$. The standard WKB approach is to seek the solution to Eqs. (3) and (4) in the form of $\tilde{a}_\pm(\tilde{z}) = a_\pm^{(0)}(\tilde{z}) e^{iS(\tilde{z})}$, where $a_\pm^{(0)}$ is slowly varying with $\tilde{z}$. If the dependence of $a_\pm^{(0)}$ and all other terms on $\tilde{z}$ is neglected, we obtain

$$\begin{pmatrix} D_+(\tilde{z},n) & g(\tilde{z}) \\ g(\tilde{z}) & D_-(\tilde{z},n) \end{pmatrix} \begin{pmatrix} a_+^{(0)} \\ a_-^{(0)} \end{pmatrix} = 0, \tag{9}$$

where $n(\tilde{z}) \equiv dS(\tilde{z})/d\tilde{z}$ is the local wave number. Note that according to Eq. (7) the physical meaning of $n(\tilde{z})$ is the wave number of the plasma wave associated with the given branch μ, where $1 \leqslant \mu \leqslant 4$, at the given point $\tilde{z}$. There are at most four branches corresponding to two helicites (RHCP and LHCP) and two propagation directions (forward and backward). At some points $\tilde{z}$ some of the branches may not exist. For example, we will show that in the intermediate pitch regime only two branches ($1 \geqslant \mu \leqslant 2$) exist in the plasma plateau region. The normalized wave number $n^{(\mu)}(z)$ is found by solving the fourth-order polynomial equation,

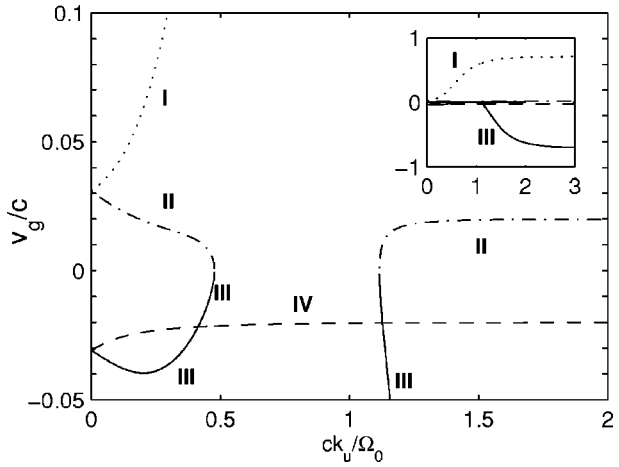

FIG. 3. Group velocity of propagating modes inside the UIT plasma (plateau region) vs the undulator wave number. The four propagation branches are labeled: right-moving LHCP (I) and RHCF (II) waves, and left-moving LHCP (III) and RHCP (IV). The inset shows the group velocities over a wider range of n_u.

$$0 = D(k,\omega,\tilde{z}) \equiv D_+(\tilde{z},n) D_-(\tilde{z},n) - g^2(\tilde{z}), \tag{10}$$

where $D_\pm(\tilde{z},n) = (n \pm n_u)^2 - n_\pm^2(\omega,\tilde{z})$ and $k = n\omega/c$. By calculating $n^{(\mu)}(\tilde{z})$'s that satisfy Eq. (10), a phase space trajectory in the $(n,\tilde{z})$ phase space can be drawn[24] for each real-valued $n^{(\mu)}$. The direction of the ray motion in the phase plane is determined by the sign of the group velocity $v_g = \partial\omega/\partial k$ at a given point $(n,\tilde{z})$ for each propagation branch. From Eq. (10), the value of the group velocity is evaluated according to

$$v_g = -\frac{\partial D/\partial k}{\partial D/\partial \omega} \tag{11}$$

for each propagation branch that exists at a given z. Inside the plateau region of the plasma, for the "perfect transparency" regime ($\omega = \Omega_0 = \overline{\omega}_p$, $B_u/B_0 = 0.2$), v_g/c is plotted in Fig. 3 as a function of the normalized undulator wave number n_u. Three regions of n_u can be identified in Fig. 3 of small and large n_u, where four different propagation branches coexist, and of intermediate n_u, where only two branches are found.

Equation (9) also provides information about the relative magnitudes of the RHCP and LHCP helicities in a given propagation branch:

$$K(\tilde{z},n) = \frac{a_-^{(0)}}{a_+^{(0)}} = -\frac{D_+(\tilde{z},n)}{g} = -\frac{g}{D_-(\tilde{z},n)}. \tag{12}$$

Taking into account the slow variation of n^μ with $\tilde{z}$, an equation for the mode amplitudes of each propagation branch can be derived. The total two-component WKB solution at a given point $\tilde{z}$ is then expressed as

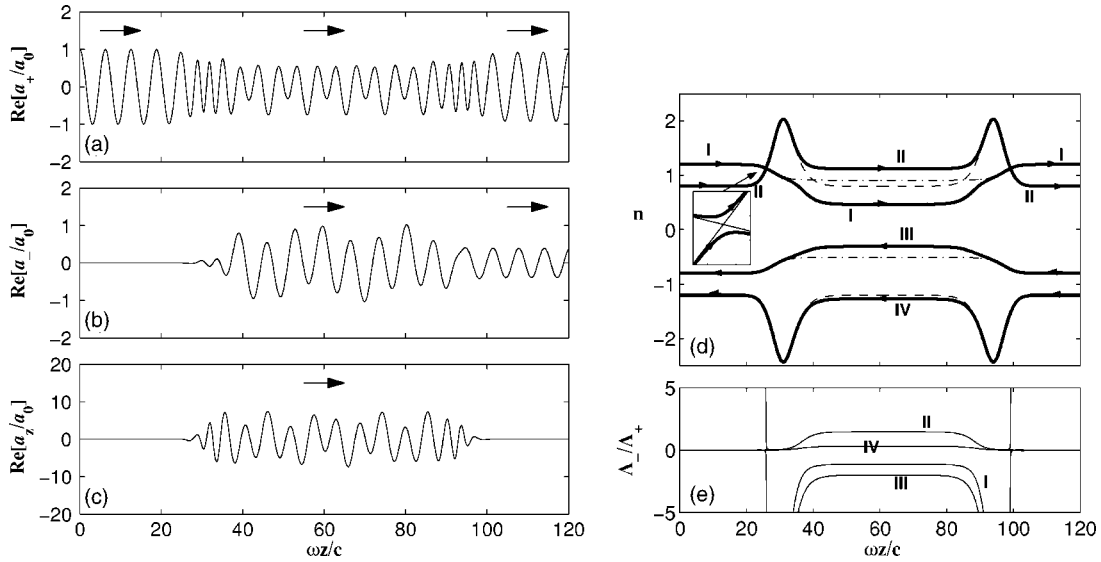

FIG. 4. Small-pitch propagation regime: $n_u=0.2$, $B_u=0.2B_0$, $\omega=\Omega_0$, $\overline{\omega}_p=\Omega_0$. Left column—amplitudes of the electromagnetic wave components in the UIT plasma normalized to that of the injected RHP wave $a_+^{\mathrm{inc}}=a_0$ obtained by solving Eqs. (3) and (4) (a) RHCP, (b) LHCP, and (c) longitudinal electric field. Arrows indicate the direction of the phase velocity. Right column: geometric optics approach to wave propagation of two coupled wave helicities. (d) Solid lines: phase space trajectories calculated from Eq. (10). Arrows indicate group velocity direction from Eq. (11). Dashed line and dot-dashed lines: noninteracting ($g=0$) forward RHCP and backward LHCP. (e) Mode ratio $|a_-/a_+|$ for the propagation branches (labeled by I–IV). Inset shows that the trajectories do not cross.

$$\begin{pmatrix}\tilde{a}_+\\ \tilde{a}_-\end{pmatrix}=\sum_{\mu}\begin{pmatrix}1\\ K\end{pmatrix}\frac{C^{(\mu)}}{\sqrt{n^{(\mu)}(1+K^2)+n_u(1-K^2)}}\times\exp\left(\int^{\tilde{z}} n^{(\mu)}d\tilde{z}\right),\tag{13}$$

where the summation is over all modes present at $\tilde{z}$, and $C^{(\mu)}$ are constants determined by the initial conditions. WKB description assumes that the existing propagation branches do not interact. Because we are dealing with electromagnetic waves and not with geometric rays, this description is only approximate. As shown in Sec. II B, WKB solutions become inaccurate if dispersion curves become close to each other in some region of the phase space. In those regions electromagnetic waves can tunnel between branches experiencing mode conversion.[24]

B. Three propagation regimes in UIT plasma

Aided by the qualitative WKB description, we can now investigate the three regimes of wave propagation in the UIT regime by solving Eqs. (3) and (4). For all cases we assume that $B_u=0.2B_0$ and that the perfect transparency condition $\omega=\Omega_0=\overline{\omega}_p$ is satisfied. Therefore, $n_+=1$ in the plasma plateau region, and in the absence of interhelicity coupling the incident from the left onto the plasma RHCP wave must transmit through the plasma. Boundary conditions at the left boundary of the computational domain ($z=0$) corresponding to the RHCP wave with amplitude a_+^{inc} incident from the left on the vacuum-plasma boundary are imposed:

$$\left[a_+ - i\frac{c}{\omega}\frac{\partial a_+}{\partial z}\right]_{z=0}=2a_+^{\mathrm{inc}},\quad \left[a_- - i\frac{c}{\omega}\frac{\partial a_-}{\partial z}\right]_{z=0}=0.\tag{14}$$

Boundary conditions at the right boundary of the computational domain ($\omega z/c=120$) ensures that there is no incident radiation from the right:

$$\left[a_+ + i\frac{c}{\omega}\frac{\partial a_+}{\partial z}\right]_{z=L}=0,\quad \left[a_- + i\frac{c}{\omega}\frac{\partial a_-}{\partial z}\right]_{z=L}=0.\tag{15}$$

First, consider the case of a small-pitch undulator, $k_u=0.2\omega/c$. The solutions of Eqs. (3) and (4) are plotted in the left column of Fig. 4; phase space trajectories in the WKB limit are plotted in the right column of Fig. 4. Figures 4(a) and 4(b) show that that even though the RHCP wave gets into the plasma, it acquires a significant LHCP component in the plasma. Figures 4(a) and 4(e) validate this conclusion. The inset in Fig. 4(d) indicates that the wave at $z=0$ along the RHCP branch labeled II is split between branches I and II inside the plasma. Because both branches I and II have almost equal a_+ and a_- components, the beat wave patterns in Figs. 4(a) and 4(b) indicate that both branches are excited. Of course, geometric optics cannot capture the coupling between branches I and II that takes place in the plasma. In the small-pitch regime there are four propagation branches inside the plasma. Only the forward-moving RHCP and LHCP are strongly coupled. The backward moving branches have very different propagation wave numbers and are not excited in the plasma. Therefore, there is no reflection from the UIT plasma visible in Fig. 4(a).

The intermediate-pitch case is analyzed in Fig. 5 for $k_u=0.9\omega/c$. In the intermediate pitch regime there are only two propagating branches inside the plasma. Coupling is strong

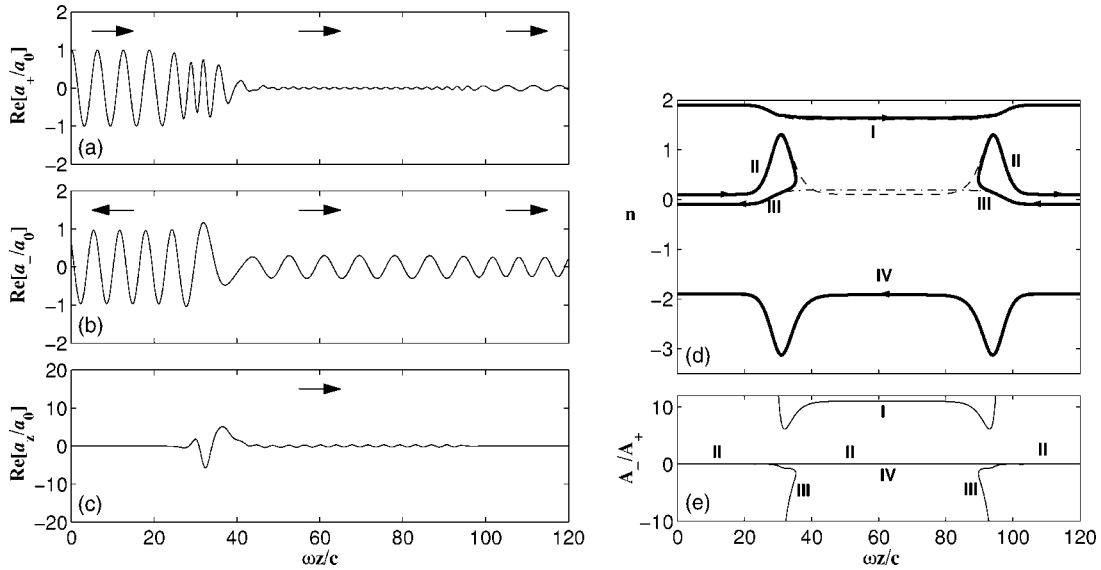

FIG. 5. Intermediate pitch regime: same as Fig. 4, but $n_u=0.9$. Injected from $z=0$ (along branch I) RHCP does not penetrate into the plasma and is reflected along branch III as LHCP.

between the forward and backward propagating waves at the entrance into the plasma. In this regime plasma is opaque to RHCP wave which does not penetrate into the plateau region. The opaqueness is caused by the strong conversion (about 90%) of the forward-traveling RHCP into the backward-traveling LHCP. The remaining 10% is mode converted into the forward-traveling LHCP which penetrates into the plateau region of the plasma, and subsequently leaves the plasma from the right side. Near the exit from the plasma this small LHCP partly converts into an even smaller RHCP which also leaves the plasma. Here and elsewhere, mode conversion coefficients have been obtained from the numerical simulations.

Longitudinal plasma wave has a very small amplitude because of the small RHCP component of the electric field in the plasma plateau region. Geometric optics calculation sketched in Fig. 5(d) confirms that interpretation: the RHCP wave injected along the branch I reflects back along the branch III as the LHCP wave. This propagation regime is useful in illustrating the lack of symmetry between the forward and backward waves. Although the RHCP wave injected from the left does not penetrate the plasma, the RHCP injected from the right does, as shown by the branch III in Fig. 5(d). Therefore, in this regime the UIT plasma serves as a "wave diode:" it transmits RHCP waves traveling in one direction and reflects those traveling in the opposite direction. As will be explained in Sec. III, this asymmetry between the forward and backward propagating waves is due to the fact that the helicity of a helical undulator is changed by the inversion transformation which interchanges forward and backward waves.

In the case of a large-pitch undulator ($k_u=1.6\omega/c$) shown in Fig. 6 we observe that the injected from the left RHCP does transmit through the plasma, with a small reflection into the LHCP wave. This reflection can be understood from the geometric optics picture by noting that branches I and II are very closely located in the phase space. This proximity increases the tunneling coefficient between the branches and results in a measurable reflection. The large pitch is the only propagation regime which is accurately described by the single-helicity theory:[17] both the forward and backward RHCP penetrate the plasma and slow down to a small group velocity $v_g \ll c$. This is well illustrated by Fig. 3 for $ck_u/\Omega_0 > 1.5$ propagation branches II and IV have approximately equal and opposite group velocities $|v_g| \approx 0.02$. Note that in all three Figs. 4–6 corresponding to small, intermediate, and large-pitch undulators, the dashed lines denoting the phase space trajectory of a forward moving RHCP in the absence of interhelicity couplingis are identical to each other. It is the interhelicity coupling that explains the difference in wave propagation for different undulator wave numbers.

III. ENGINEERING PROPAGATION PROPERTIES OF ELECTROMAGNETIC WAVES NEAR CYCLOTRON RESONANCE

Although energy compression is one the most appealing applications of UIT, we have found another interesting application that does not require a small group velocity. UIT enables engineering propagation properties of electromagnetic waves in the vicinity of the cyclotron resonance that is very counterintuitive and, at the same time, desirable for high power microwave applications. One example considered by us is engineering of a microwave propagation band with a nonvanishing group velocity for vanishing wave number $k_+ \equiv k+k_u$ of the RHCP wave component. This is indeed a highly desirable propagation property because it can lead to efficient broadband generation of microwaves in a relativistic beam driven microwave device such as a gyrotravelling wave tube (gyro-TWT).[21] Efficiency increase comes from the smallness of the wave number k_+ whereas the broadband characteristic comes from the possibility of matching the electron beam velocity v_b and microwave group velocity v_g.

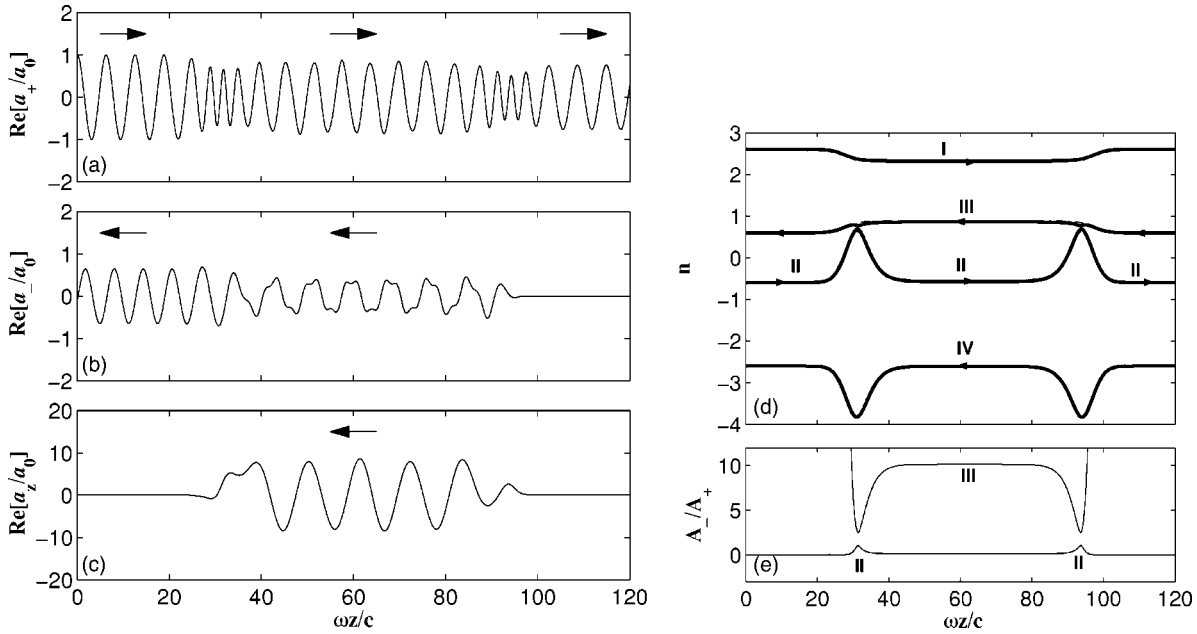

FIG. 6. Large pitch propagation regime: same as Fig. 4, but $n_u=1.6$. Injected from $z=0$ RHCP transmits through the plasma. Single-helicity theory is fairly accurate in this regime.

A smooth waveguide does not allow for simultaneous $k_+=0$ and large group velocity. The present solution is to make a helically corrugated waveguide.[21]

Adding plasma to high power microwave devices has been credited with increasing the electron beam current, bandwidth, efficiency, and reducing the need for guiding magnetic fields.[27] To increase the bandwidth it is beneficial to find the regime in which a plasma-filled device supports waves with $d\omega/dk=v_b$ for $k_+=0$. Because in any medium with inversion symmetry $\omega(k_+)$ is an even function of k_+, a medium with a broken inversion symmetry must be identified. UIT plasma is such a medium. To see that there is an asymmetry between forward $(k_+>0)$ and backward $(k_+<0)$ waves, consider the inversion transformation $(z\rightarrow -z)$ that exchanges the forward and backward waves. Inversion does not affect the axial magnetic field B_0e_z because magnetic field is a pseudoscalar. However, the undulator helicity $H=\mathbf{A}_u\cdot\mathbf{B}_u$ does change its sign. Hence, the presence of an undulator causes the asymmetry between the forward and backward waves and makes the UIT plasma a medium without inversion symmetry. One of the manifestations of this asymmetry has already been described in Sec. II B (see Fig. 5) where only the backward traveling RHCP waves were transmitting through the plasma at $\omega=\Omega_0$.

In Fig. 7 the dispersion relation ω vs k_+ is shown for $B_u=0.2B_0$, $k_u=-0.35\Omega_0/c$ (negative helicity undulator), and $\Omega_0=\overline{\omega}_p$ (perfect transparency condition). This dispersion relation is obtained by solving Eq. (10) inside the plasma plateau region and using $k_+=k+k+u$. Figure 7(b) is a blow-up of Fig. 7(a) for small wave numbers k_+ clearly showing two branches with a positive group velocity at $k_+=0$. The exact values of the group velocities and the corresponding to $k_+=0$ "cutoff" frequencies can be easily tuned by varying the undulator pitch and strength. Because we are interested in the frequencies detuned from the exact cyclotron resonance,

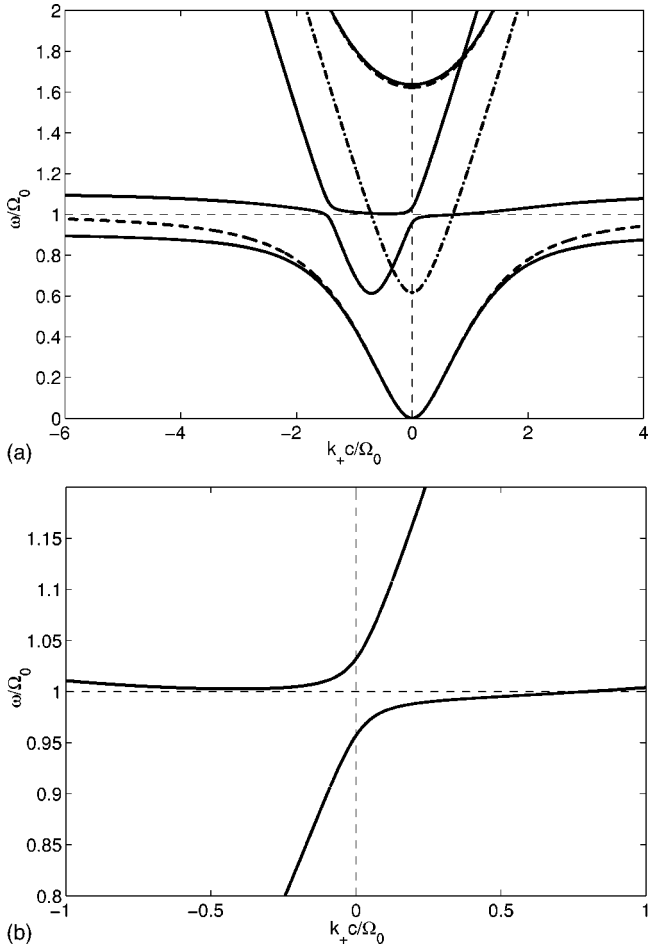

FIG. 7. (a) Solid lines: dispersion relation ω/Ω_0 vs ck_+/Ω_0 for $B_u=0.2B_0$, $k_u=-0.35\Omega_0/c$ (negative helicity undulator), and $\Omega_0=\overline{\omega}_p$ (perfect transparency condition). Dashed lines: dispersion characteristics of the RHCP and LHCP waves in a magnetized plasma without an undulator. (b) Blow-up of (a) for small wave numbers demonstrating the nonvanishing group velocity $v_g=d\omega/dk>0$ for $k=0$.

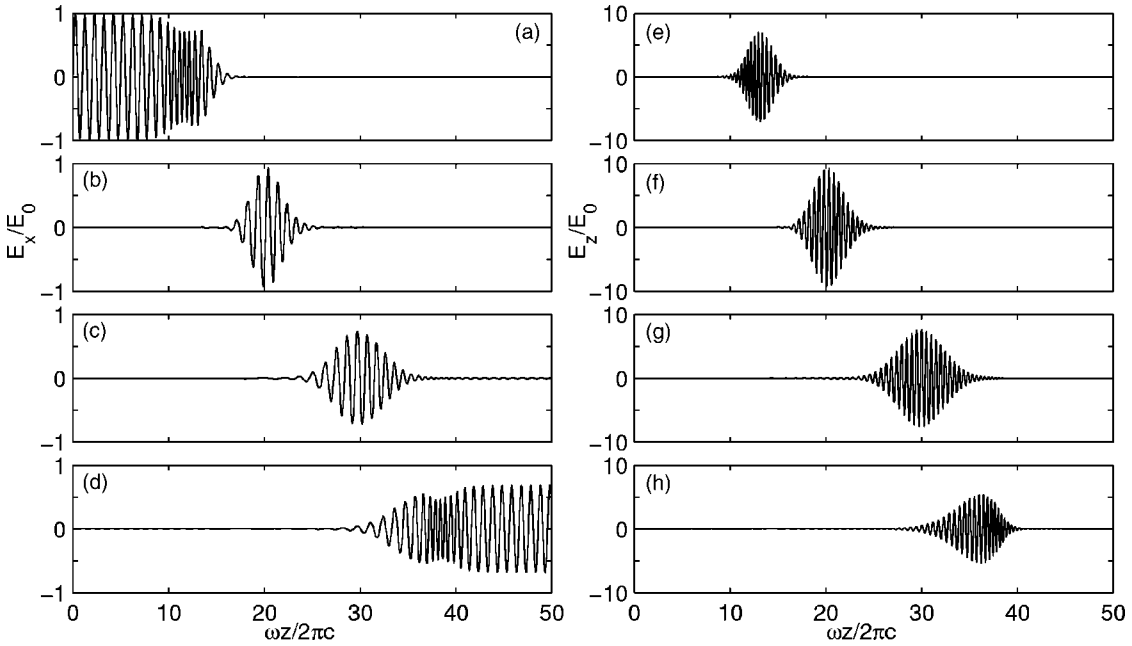

FIG. 8. Sequential snapshots at $t=t_i$ of the time evolution of the transverse [left column, (a)–(d)] and longitudinal [right column, (e)–(h)] electric field normalized to the peak electric field in the incident wave $a_+^{\mathrm{inc}}=10^{-3}$. Undulator parameters: $n_u=1.6$, left helicity. (a) and (e), $t_1=216\lambda/c$; (b) and (f), $t_2=600\lambda/c$; (c) and (g), $t_3=1104\lambda/c$; and (d) and (h), $t_4=1488\lambda/c$.

group velocity can be fairly high and the transverse electric field component comparable to the longitudinal component. This is in contrast to the $\omega=\Omega_0$ case corresponding to slow waves with the dominant longitudinal electric field.

IV. ENERGY COMPRESSION FOR ACCELERATOR APPLICATIONS

The results of the linearized single-frequency fluid simulations presented in Sec. II B predict significant energy compression in the large-pitch undulator regime. For several reasons, it is important to verify these results using first-principles time-dependent fully relativistic particle simulations. First, for $B_u \ll B_0$ UIT is a very narrow-band phenomenon, and it is important to know how it is manifested for finite duration pulses. Second, it has been demonstrated[18] that nonlinear relativistic effects become important in UIT even for the subrelativistic wave amplitudes $e|\mathbf{E}|/mc\omega \ll 1$. And, finally, it is important to understand the spatial and temporal resolution requirements for modeling UIT with a PIC simulation. The one-dimensional version of the fully electromagnetic relativistic PIC code VLPL (Ref. 28) was used for this study. The following simulation parameters have been used: grid size $\delta z=0.025\lambda$ (where $\lambda=2\pi c/\omega$ is the vacuum wavelength of the incident radiation), $\delta t=0.95\delta z/c$, 128 particles per cell. The incident circularly polarized probe pulse has the Gaussian envelope $a=a_+^{\mathrm{inc}}\exp[-(\omega z/c-\omega t)^2/T^2]$ with the duration $T=100\lambda/c$ and peak amplitude $a_+^{\mathrm{inc}}=10^{-3}$. The large undulator wave number $k_u=1.6\Omega_0/c$ ensures plasma transparency and significant energy compression for both propagation directions.

The electron plasma density profile is chosen to have a smooth vacuum/plasma interface and a constant-density plateau region $15<z/\lambda<35: N(z)/N_0=0.5\tanh[(z/\lambda-10)/1.67]-0.5\tanh[(z/\lambda-40)/1.67]$. The axial magnetic field has the magnetic trap shape: gradually decreasing from a high amplitude ($eB_z/mc=2\omega$) in the low plasma density regions to the perfect UIT value of $eB_0/mc\equiv\Omega_0=\omega$ in the plasma plateau region: $B_z/B_0=2-0.5\tanh[(z/\lambda-10)/1.67]+0.5\tanh[(z/\lambda-40)/1.67]$. The results of ID PIC simulations for the undulator with $n_u=-1.6$ are shown in Fig. 8. These simulations physically correspond to the case of $n_u=1.6$ illustrated by Fig. 6(d), with the incident RHCP wave traveling from right to left. The transverse E_x and longitudinal E_z components of the electric field are plotted as different time snapshots corresponding to the incident pulse just entering the vacuum/plasma interface ($t=216\lambda/c$), being totally compressed in the plasma ($t=600\lambda/c$), reaching the far end of the plasma ($t=1104\lambda/c$), and exiting the plasma ($t=1488\lambda/c$). All fields are normalized to incident field amplitude. As shown in the right panel in Fig. 8, the longitudinal electric field is ten times stronger than the transverse electric field approximately equal to that of the incident wave. Therefore, energy compression by a factor of 50 is observed. The phase velocity of the longitudinal field is subrelativistic: $v_{ph}\approx 0.4c$, making it attractive for ion acceleration.

Simulations result for the undulator with $n_u=1.6$ are shown in Fig. 9. These simulations physically correspond to the case of $n_u=1.6$ illustrated by Figs. 6(a)–6(d), with the incident RHCP wave traveling from left to right. Here too we observe energy compression by about the same factor. Some reflection from the plasma is observed. We contribute this reflection to partial conversion from forward traveling RHCP to backward traveling LHCP as illustrated by Figs. 6(b), 6(d), and 6(e). Note that the steady state reflection coefficient deduced from Fig. 6(b) is significantly larger than observed in time-dependent simulations. We speculate that this reduc-

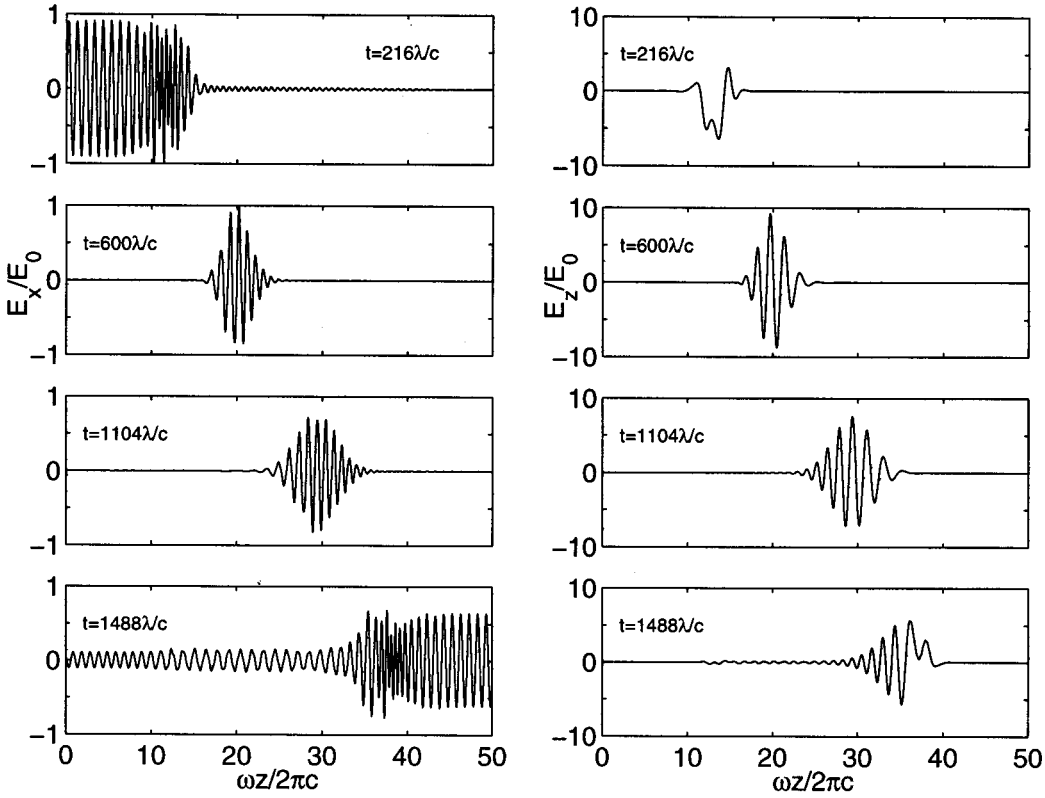

FIG. 9. Same as Fig. 8 but with $n_u=1.6$ (right undulator helicity).

tion in reflection revealed by the PIC simulations is a finite pulse duration effect alluded to earlier. The phase velocity of the longitudinal plasma wave is $v_{ph}=-1.6c$. By increasing the undulator wave number to $n_u=2.0$ one can reduce the phase velocity to $v_{ph}=-c$ making it attractive for electron acceleration.

In summary, we have demonstrated that propagation of electromagnetic waves near the electron cyclotron resonance frequency can be dramatically modified by the addition of a helical magnetic undulator. Specifically, plasma can be made electromagnetically transparent at and near the electron cyclotron resonance frequency through the undulator induced transparency (UIT). UIT enables extreme compression of electromagnetic energy in the plasma by slowing down electromagnetic waves to the group velocity much smaller than the speed of light in vacuum. Thus compressed electromagnetic waves can be used for electron and ion accelerations. Coupling between two radiation helicites, right-hand circular polarization (RHCP) and left-hand circular polarization (LHCP), is very essential in determining the degree, and even the very fact of energy compression. This coupling also enables engineering wave propagation properties for small wave numbers. By a judicious choice of undulator period and strength group velocity of the wave can be made finite for $\vec{k}=0$. This has potential applications to beam-driven high power microwave generation by gyro-TWTs.

ACKNOWLEDGMENTS

This work was supported by the U.S. Department of Energy under the Contract Nos. DE-FG02-04ER54763 and DE-FG02-04ER41321 and by the Russian Foundation for Basic Research Grant No. 03-02-17234.

[1] K. J. Boller, A. Imamoglu, and S. Harris, Phys. Rev. Lett. **66**, 2593 (1991).
[2] S. E. Harris, Phys. Today **50** (7), 39 (1997).
[3] J. P. Marangos, J. Mod. Opt. **45**, 471 (1998).
[4] A. B. Matsko, O. Kocharovskaya, Y. Rostovtsev, G. R. Welch, A. S. Zibrov, and M. O. Scully, *Advances in Atomic, Molecular, and Optical Physics* (Academic, New York, 2001); Adv. At., Mol., Opt. Phys. **46**, 191 (2001).
[5] A. V. Turukhin, V. S. Sudarshanam, M. S. Shahriar, J. A. Musser, B. S. Ham, and P. R. Hemmer, Phys. Rev. Lett. **88**, 023602 (2002).
[6] S. Chesi, M. Artoni, G. C. L. Rocca, F. Bassani, and A. Mysyrowicz, Phys. Rev. Lett. **91**, 057402 (2003).
[7] L. V. Hau *et al.*, Nature (London) **397**, 594 (1999).
[8] C. Liu, Z. Dutton, C. H. Behroozi, and L. V. Hau, Nature (London) **409**, 490 (2001).
[9] D. Phillips, A. Fleischhauer, A. Mair, R. Waslworth, and M. D. Lukin, Phys. Rev. Lett. **86**, 783 (2001).
[10] O. Kocharovskaya, Y. Rostovtsev, and M. O. Scully, Phys. Rev. Lett. **86**, 628 (2001).
[11] M. Fleischhauer and M. D. Lukin, Phys. Rev. Lett. **84**, 5094 (2000).
[12] M. Fleischhauer, S. F. Yelin, and M. D. Lukin, Opt. Commun. **179**, 395 (2000).
[13] M. D. Lukin, S. F. Yelin, and M. Fleischhauer, Phys. Rev. Lett. **84**, 4232 (2000).
[14] U. Leonhardt and P. Piwnicki, Phys. Rev. Lett. **84**, 822 (2000).
[15] A. B. Matsko, Y. V. Rostovtsev, M. Fleischhauer, and M. O. Scully, Phys. Rev. Lett. **86**, 2006 (2001).
[16] A. G. Litvak and M. D. Tokman, Phys. Rev. Lett. **88**, 095003 (2002).
[17] G. Shvets and J. S. Wurtele, Phys. Rev. Lett. **89**, 115003 (2002).
[18] G. Shvets and M. Tushentsov, J. Mod. Opt. **50**, 2583 (2003).
[19] M. Hur, J. Wurtele, and G. Shvets, Phys. Plasmas **10**, 3004 (2003).
[20] A. Y. Kryachko, A. G. Litvak, and M. D. Tokman, Nucl. Fusion **44**, 414 (2004).
[21] G. G. Denisov, V. L. Bratman, A. W. Cross, W. He, A. D. R. Phelps, K.

Ronald, S. V. Samsonov, and C. G. Whyte, Phys. Rev. Lett. **81**, 5680 (1998).
[22]M. Tushentsov, G. Shvets, A. Kryachko, and M. Tokman, "Undulator-Induced Transparency of Magnetized Plasma: New Approach to Electromagnetic Energy Compression," IEEE Trans. Plasma Sci. (in press).
[23]V. Ginzburg, *The Propagation of Electromangetic Waves in Plasmas* (Pregamon, Oxford, 1970).
[24]A. N. Kaufman and L. Friedland, Phys. Lett. A **123**, 387 (1987).
[25]R. Cairns and C. Lashmore-Davies, Phys. Fluids **26**, 1268 (1983).
[26]A. N. Kaufman, H. Ye, and Y. Hui, Phys. Lett. A **120**, 327 (1987).
[27]D. M. Goebel, Y. Carmel, and G. S. Nusinovich, Phys. Plasmas **6**, 2225 (1999).
[28]A. M. Pukhov, Bull. Am. Phys. Soc. **41** (7), 1502 (1996).